EFFECTS OF SPECIMEN GEOMETRY ON ELASTIC-PLASTIC R-CURVES FOR Zr - 2.5% Nb

L. A. Simpson

Atomic Energy of Canada, Ltd.
Whiteshell Nuclear Research Establishment
Pinawa, Manitoba, ROE 1LO, Canada

ABSTRACT

Crack-growth resistance curves, for Zr-2.5% Nb pressure tubing, are determined from measurements of crack opening displacement and J-integral during stable crack extension in center-cracked tensile specimens. These are used, in conjunction with crack-drive curves for a cracked pressure tube, to predict critical crack length. The resulting predictions are more accurate than those made using compact tension specimens in an earlier paper. The geometry dependence of R-curve shape is discussed in terms of recent theoretical results. The contribution of shear lip formation to R-curve behavior is also discussed using results on side-grooved specimens.

KEYWORDS

R-curve; J-integral; crack opening displacement, critical crack length; zirconium

INTRODUCTION

Recent studies, in this laboratory (Simpson and Clarke, 1979; Simpson and Wilkins, 1979), have been concerned with developing a fracture mechanics framework for predicting the critical crack length in reactor pressure tubes, using tests on small specimens. The pressure tube material is cold-worked Zr-2.5% Nb, which provides the primary coolant containment in the CANDU[1] nuclear reactor system. Zr-2.5% Nb can tolerate considerable stable crack extension under rising load, following crack initiation. In fact, Simpson and Wilkins (1979) showed that the pressure for unstable propagation of a pressure tube crack can exceed that for initiation by a factor of three. Hence, if this material is to be efficiently utilized in design, the only sensible fracture criterion is one which takes advantage of this property, such as an R-curve approach.

To establish a predictive framework, Simpson and Wilkins (1979) cut compact tension (CT) specimens directly from pressure tube material, which had previously been slit axially and burst-tested. The crack-growth resistance was determined using compact tension (CT) specimens, and expressed in terms of the crack-opening displacement (COD) at the actual crack tip and, the J-integral. The critical crack length for

[1] CANada Deuterium Uranium

a pressure tube was then determined by comparing an R-curve to a plot of crack driving force against crack length for the parent pressure tube, loaded to the previously determined burst pressure. The predicted critical crack length was compared with the actual slit length in the parent pressure tube. The predicted values were slightly conservative (underestimated the critical crack length) but were not so low as to unduly penalize the material, as would a criterion based on initiation. If it could be demonstrated that predictions from a CT specimen will always be conservative, then this approach would be useful in design. To do this, we must understand the factors which are responsible for the crack-growth resistance and the way in which these factors depend on specimen geometry.

Specimen Geometry and Crack Growth Resistance

In our first paper (Simpson and Clarke, 1979), R-curve shape was shown to be insensitive to crack length and specimen size for the CT specimen. While this gave initial encouragement that R-curves might be geometry independent, the direct comparisons with pressure tube burst-tests by Simpson and Wilkins (1979) suggested otherwise. About the same time, other workers were arriving at similar conclusions. Garwood (1979) compared R-curves (based on both COD and J) for bend specimens with curves for center cracked tension (CCT) specimens cut from pipeline steel. The CCT R-curves were considerably steeper than those for the bend specimens. This difference was tentatively attributed to larger shear lips present in the CCT specimens. Shih, de Lorenzi and Andrews (1979) tested both CT and CCT specimens of A533B steel. While both J and COD-based R-curves were obtained for CT specimens, crack extension in the CCT specimens initiated and progressed along shear bands at 45° to the original crack plane. Clearly, the crack-tip deformation state was very different from the CT specimen and R-curves plotted from such CCT data would be expected to be different from those obtained from CT specimens.

In this work the CCT specimen has also been chosen as an alternate geometry, mainly because it represents the closest replication of the actual pressure tube crack. R-curves are constructed from measurements of J and COD and compared with the previous results for CT specimens. Secondly, we examine the mechanism of increasing crack-growth resistance itself, by attempting to separate that portion of the resistance due to shear lip formation from that portion intrinsic to the material. Shear lip formation is suppressed by testing side-grooved specimens.

EXPERIMENTAL

CCT Specimens

CCT specimens, Fig. 1, were cut from flattened, 10.7 cm dia., pressure tubing such that the crack was in the axial direction of the tube. They were slightly less than full thickness (4.1 mm) due to surface machining and were slit by spark machining. The slits were sharpened by fatigue cycling to maximum values of stress intensity factor of less than one half that required for crack initiation. Crack extension was monitored by an electrical potential method (Johnson, 1965) and COD at the actual crack tip was determined by a method similar to that used in our previous papers for CT specimens. Displacements along the complete specimen width were measured by photographing two rows of microhardness indentations, one above and one below the crack plane. By measuring the separation of opposite pairs of indentations, a displacement profile was obtained. This is an approximate measure of the total work-producing displacement undergone by the material near the crack plane, including the entire plastic zone. Its value at the position of the actual crack tip was taken as our definition of COD. R-curves were generated from simultaneous readings of load, displacement and crack extension, made at frequent intervals throughout the test.

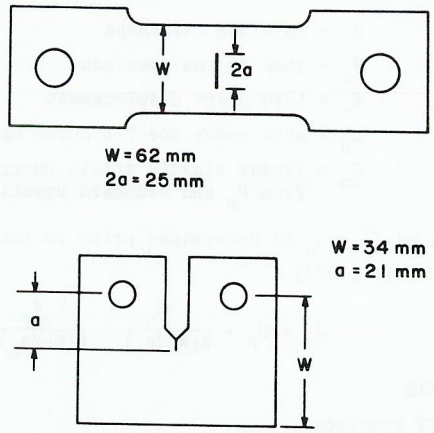

Fig. 1. Specimen sizes used in this study.

Side-Grooved Specimens

A number of CT specimens, similar to those used by Simpson and Wilkins (1979) (W = 34 mm, a/w = 0.6) were grooved to a depth of about 20% of the thickness, in the crack plane, on each side. R-curves were determined by the method described in the above paper at 240°C and 20°C. One CCT specimen was also grooved and tested at 20°C.

R-Curve Determination

To facilitate comparison of COD-based R-curves with crack-driving-force curves, the crack-growth resistance was expressed in units of stress intensity factor, K_R, where

$$K_R = (m \cdot \delta \cdot E \cdot \sigma_y)^{1/2} \qquad (1)$$

and

δ = COD

σ_y = yield strength

E = Young's modulus.

m is a constant which previous work (Simpson, 1980) suggests is close to unity.

The J-integral after crack extension was calculated incrementally using an approach established by Garwood, Robinson and Turner (1975). This was derived for a CT specimen and used the areas under the "equivalent" non-linear-elastic load-deflection curves for the specimen after successive, small increments of crack extension. The application of this procedure to our CT specimens is described in Simpson and Wilkins (1979). An entirely similar approach can be applied to a CCT specimen to derive the following equations for J_n, after the n^{th} increment of crack extension.

$$J_n = J_{n-1}\frac{W-2a_n}{W-2a_{n-1}} + G_n\frac{W-2a_n}{W-2a_{n-1}} - G_{n-1} + \frac{2(U_n-U_{n-1})}{B(W-2a_{n-1})} - \frac{P_n\delta_n - P_{n-1}\delta_{n-1}}{B(W-2a_{n-1})} \qquad (2)$$

where

B = specimen thickness

P_n = load on the specimen

δ_n = load point displacement

U_n = area under the P-δ curve up to the n^{th} increment

G_n = linear elastic strain energy release rate calculated from P_n and standard equations in Tada (1973).

The initial value of $J_n = J_o$ is determined prior to initiation and is given by Rice, Paris and Merkle (1973)

$$J_o = G_o + \frac{2U_o}{B(W-2a_o)} - \frac{P_o\delta_o}{B(W-2a_o)} \qquad (3)$$

RESULTS

Full Thickness CCT Specimens

Because of difficulties, inherent to testing CCT specimens, only two out of eleven tests yielded results which were considered useable. The main difficulty was in obtaining symmetrical crack extension at both ends of the crack. When the cracks grew at unequal rates the analysis was invalidated. Contrary to work cited earlier (Garwood, 1979; Shih, Lorenzi and Andrews, 1979), the proportion of shear lip in the CCT specimens was not noticeably different from the CT specimens, nor did the crack deviate from its original direction of propagation.

R-curves for two successfully tested specimens are plotted in terms of both J (J_R) and COD (K_R) in Figs. 2 and 3 respectively. Also included are the corresponding curves for CT specimens from our earlier work (Simpson and Wilkins, 1979). The COD data was analyzed separately for each end of the crack. The scatter for COD data was quite large, especially during the initial stages of the test. For this reason, the J_R curves, which were computed using the larger load-line displacements, were considered more reliable.

Following the procedure used by Simpson and Wilkins (1979), the R-curves in Figs. 2 and 3 were used to predict critical crack length in a pressure tube, by comparing them with plots of crack driving force (CDF) against crack length for a cracked tube. The expressions used for CDF were

$$J_{CDF} = \frac{K^2_{CDF}}{E} = \frac{8a\bar{\sigma}^2}{E\pi} \ell n \left(\sec \frac{\pi M \sigma_H}{2\bar{\sigma}}\right) \qquad (4)$$

where

$\bar{\sigma}$ = flow stress = $(\sigma_u + \sigma_y)/2$

σ_H = applied hoop stress in tube

M = curvature-stress magnification factor

This is essentially a linear elastic expression containing a correction to the crack length to account for the plastic zone. The burst pressures determined in three burst-test experiments were used to determine σ_H. The critical crack length predictions are compared with the actual crack length values, 2a, and the previous CT results, in Table 1.

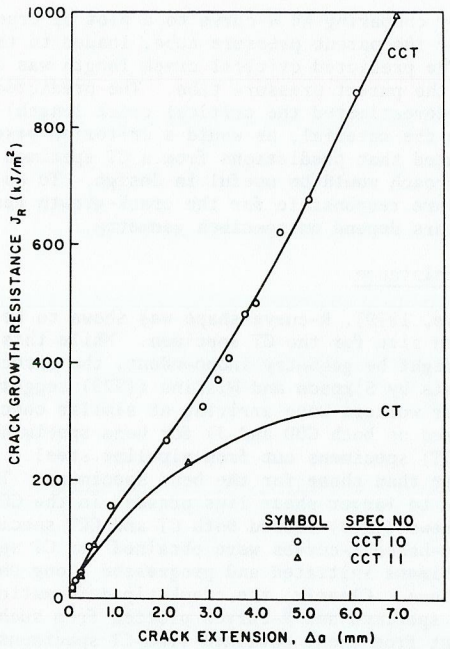

Fig. 2. J_R data for CCT specimens compared with previous CT results.

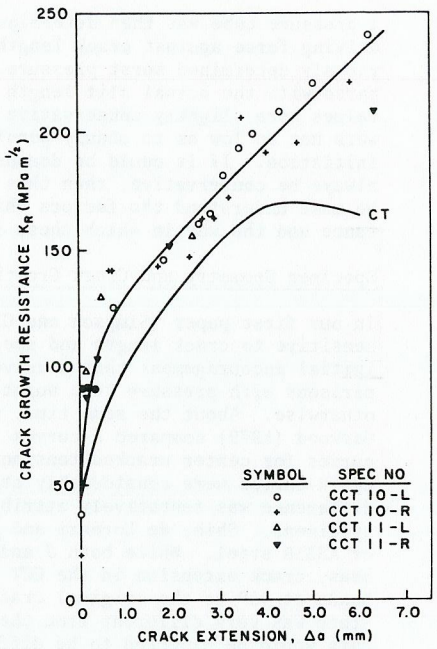

Fig. 3. K_R (COD) data for CCT specimens compared with previous CT results.

Table 1. Summary of Critical Crack Length Predictions

Tube No.	$\bar{\sigma}$	σ_H	2a	CT Pred.		CCT Pred.	
				COD	J	COD	J
	MPa	MPa	mm	mm	mm	mm	mm
27	834	481	24.5	17	18	21	24
5	791	317	44.8	35	38	39	44
15	864	242	74.4	44	42	54	62

Three main points arise from these results. First, the CCT specimens predict larger critical crack lengths than the CT specimens. Secondly, the J_R curves predict critical lengths which are essentially identical to the actual values for the two shortest cracks. (The specimens were cut from tube number 27). The error for the longer crack may be associated with uncertainties in M (Eqn. 4) at large crack sizes. Finally, the agreement between the J and COD based predictions using CCT specimens is not as good as for the CT experiments.

Side Grooved Specimens

Following initiation, COD measured on side grooved specimens was considerably smaller than on full thickness specimens and hence more difficult to measure accurately. Therefore only the J_R-curves are presented here. At 240°C, side-grooved CT specimens still showed a substantial increase in crack-growth resistance with Δa although, it was considerably less than for full thickness specimens, Fig. 4.

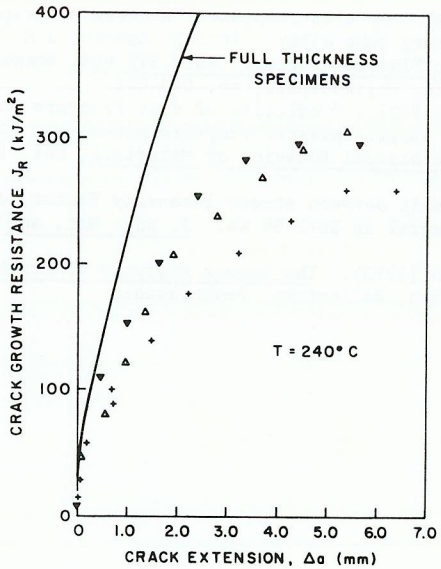

Fig. 4. Results for side-grooved specimens at 240°C.

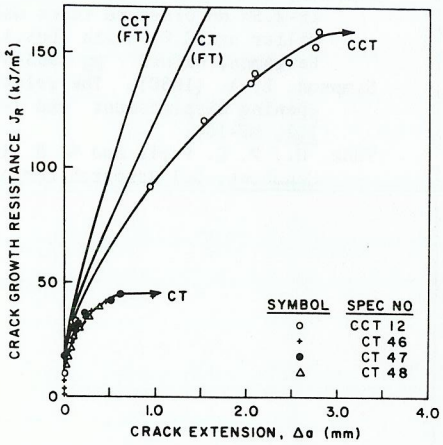

Fig. 5. Results for side-grooved specimens at 20°C (FT = Full Thickness)

CT specimens tested at 20°C with side grooves tended to become unstable after very little crack extension, Fig. 5. The CCT specimen also became unstable quickly. Because of this, it was not possible to check the crack-length calibrations and some uncertainty exists in these measurements, especially for the CCT test. The R-curves for 20°C are given in Fig. 5 along with the initial portions of the full thickness curves. While some intrinsic R-curve behavior exists at 20°C, clearly most of the increase in crack-growth resistance is due to shear lip formation.

DISCUSSION

Geometry Dependence of the Resistance Curves

Clearly, since the CCT based R-curves are considerably steeper than those for the CT specimens, the resistance curve cannot be considered to be a universal fracture parameter. However, an understanding of this geometry effect may still permit the application of this approach to fracture prediction. Reference to the evolving theories of elastic-plastic resistance curve concepts is enlightening. In the Hutchinson and Paris (1979) treatment, the HRR field, which describes the deformation state at a stationary crack tip (and describes J-dominated conditions), is assumed to move through the material with the advancing tip. The condition for validity of this concept is that the non-proportional strain increments near the tip are small in comparison with the proportional parts. Stated quantitatively, this demands

$$\omega = \frac{b}{J}\frac{dJ}{da} >> 1 \qquad (5)$$

where b = W-a for CT, and (W-2a)/2 for CCT.

Exactly how large this inequality must be has not been clearly established, but current opinions suggest that it should be at least an order of magnitude. With

ligament sizes b ≈ 15 mm and dJ/da ≈ 140 MJ/m^3, this criterion is violated when J > 210 kJ/m^2 for the CCT specimen. In a finite element study, McMeeking and Parks (1979) examined the minimum ligament size in CCT and bend-type (CT) specimens for ensuring that the near-tip fields were J-dominated. They concluded that

$$b > 25\ J/\sigma_y \text{ for CT} \quad \text{and} \quad b > 200\ J/\sigma_y \text{ for CCT}, \qquad (6)$$

reflecting the considerably lower amount of constraint in CCT specimens. In our CCT specimens this requirement is violated for J > 60 kJ/m^2 whereas in our earlier work on CT specimens (b ∿ 10 mm) J dominance would have persisted up to J ≈ 300 kJ/m^2. The two curves in Fig. 2 diverge significantly at J ≈ 60-80 kJ/m^2, which is consistent with the above limits. Thus, after less than 1 mm of crack extension, the significance of the parameter we call J becomes unclear. In spite of this fact, and the fact that the tangency point between R-curve and CDF curve occurs after several mm of crack extension, the critical crack length predictions are surprisingly good for the CCT specimen.

The recently published (Simpson, 1980) relationship between J_R and COD (δ), as we have defined them, is relevant here.

$$J_R = \bar{\sigma}\,\delta \qquad (7)$$

This is identical to the expression for the J-integral calculated for the Dugdale model of a crack with a plastic zone (Rice, 1968) since, δ is essentially the total work-producing displacement of the plastic zone boundaries. Therefore J_R, as measured here, appears to be associated with the total plastic work per unit crack extension. The crack driving force, as defined here, is the available energy release rate for crack extension so that a balance between this and the dissipation rate is satisfied by the tangency condition. It is therefore not surprising that for similar geometries, i.e. CCT specimen and cracked tube, the critical crack length determinations are close. Because the CT specimen provides more constraint at the crack tip, the plastic zone will be smaller and resistance curves will consequently be less steep. Thus the CT specimen should always give a conservative estimate of critical crack length.

Side-Grooved Specimens

Rice, Drugan and Sham (1980) have developed an elastic-fully plastic analysis of plane-strain, stable crack-growth in which a Prandtl slip line field moves through the material with the crack tip. Since plane-strain conditions should prevail, at least in the critical stages of our tests on side-grooved specimens, it is useful to apply this treatment to our results. Their treatment begins by deriving an expression for the crack-tip profile which includes J, defined only as a measure of loading. By assuming that the crack advances with a fixed profile (or crack-opening angle), an expression for the steady-state value of J under small-scale yielding conditions, is derived,

$$J_{ss} = J_{IC} \exp\left(\frac{\alpha T_o}{\beta}\right) \qquad (8)$$

where $T_o = \frac{E}{\sigma_y^2}\left(\frac{dJ}{da}\right)_o$ and $\left(\frac{dJ}{da}\right)_o$ = initial value of dJ/da and α,β = constants = 0.65 and 5.08 respectively.

The initial value of the tearing modulus, T_o, for the side-grooved CT specimen at 20°C is 6.3 and J_{IC} is 25 kJ/m^2. This leads to J_{ss} = 56 kJ/m^2 compared with the

experimental value (Fig. 5) of 46 kJ/m^2. Considering the sensitivity of Eqn. 8 to α/β and the uncertainty of its true value, this must be considered to be good agreement. At 240°C, $T_o \approx 30$ and J_{IC} = 30 kJ/m^2, giving J_{ss} = 1300 kJ/m^2, much above the value of 300 kJ/m^2 in Fig. 4. This may reflect a breakdown of either the plane strain conditions or small-scale yielding in the 240°C tests.

The higher steady state value for the CCT specimen in Fig. 5 may also reflect the much lower degree of constraint in the specimen (the Prandtl field is not appropriate for the CCT geometry).

SUMMARY

1. The geometry dependence of the resistance curves is consistent with current theories and experiments.
2. The CCT specimen, which is closest in configuration and deformation mode to the cracked pressure tube, also gives the best predictions of critical crack length.
3. The CT specimen is much simpler to handle experimentally and is expected to give a conservative estimate of critical crack length.
4. At 20°C most of the crack-growth resistance is due to shear lip formation while at 240°C up to 50% is intrinsic to the material.

ACKNOWLEDGEMENTS

This paper was written while the author was on sabbatical leave at Brown University. Support of the Materials Research Laboratory is gratefully acknowledged. Thanks are also due to C. F. Clarke of AECL for experimental assistance and J. R. Rice of Brown for useful discussions.

REFERENCES

Garwood, S. J. (1979). The effect of specimen geometry on crack growth resistance. In C.W. Smith, (Ed.), Fracture Mechanics ASTM STP 677, American Society for Testing and Materials, Philadelphia.

Garwood, S. J., J. N. Robinson and C. E. Turner (1975). The measurement of crack growth resistance curves (R-curves) using the J-integral. Int. J. of Fracture, 11, 528-530.

Hutchinson, J. W. and P. C. Paris (1979). Stability analysis of J-controlled crack growth. In J.D. Landes, J.A. Begley and G.A. Clarke, (Eds.), Elastic Plastic Fracture, ASTM STP 668, American Society for Testing and Materials, Philadelphia. pp. 37-64.

Johnson, H. H. (1965). Calibrating the electrical potential method for studying slow crack growth. Mater. Res. and Standards, 5, 442-445.

McMeeking, R. M. and D. M. Parks (1979). On criteria for J-dominance of crack tip fields in large scale yielding. In J.D.Landes, J.A. Begley and G.A. Clarke, (Eds.), Elastic Plastic Fracture, ASTM STP 668, American Society for Testing and Materials, Philadelphia. pp. 175-194.

Rice, J. R. (1968). In H. Liebowitz (Ed.), Fracture, Vol. II, Academic Press, New York. Chap. 3, pp. 233-236.

Rice, J. R., P. C. Paris and J. G. Merkle (1973). Some further results of J-integral analysis and estimates. In J. G. Kaufman, (Ed.), Progress in Flaw Growth and Fracture Toughness Testing, ASTM STP 536, American Society for Testing and Materials, Philadelphia. pp. 231-235.

Rice, J. R., W. J. Drugan and T. L. Sham (1980). Elastic-plastic analysis of growing cracks. Proceedings of 12th National Symposium on Fracture Mechanics, St. Louis, to be published as an ASTM special technical publication.

Shih, C. F., H. G. deLorenzi and W. R. Andrews (1979). Studies on crack initiation and stable crack growth. In J.D. Landes, J.A. Begley and G.A. Clarke, (Eds.), Elastic Plastic Fracture, ASTM STP 668, American Society for Testing and Materials, Philadelphia. pp. 65-120.

Simpson, L. A. and C. F. Clarke (1979). An elastic-plastic R-curve description of fracture in Zr-2.15% Nb pressure tube alloy. In J.D. Landes, J.A. Begley, and G.A. Clarke, (Eds.), Elastic Plastic Fracture, ASTM STP 668, American Society for Testing and Materials, Philadelphia, pp. 643-662.

Simpson, L. A. and B. J. S. Wilkins (1979). Prediction of fast fracture in Zr-2.5% Nb pressure tubes using elastic-plastic fracture mechanics. In K.J. Miller and R.F. Smith (Eds.), Mechanical Behavior of Materials, Vol. III, Pergamon, Oxford. pp. 563-572.

Simpson, L. A. (1980). The relationship between stress intensity factor, crack opening displacement and J-integral in Zr-2.5% Nb. J. Eng. Mat. and Tech., 102, 97-100.

Tada, H., P. C. Paris and G. R. Irwin (1973). The Stress Analysis of Cracks Handbook, Del Research Corporation, Hellertown, Pennsylvania.